

# Charge Noise in Liquid-Gated Single-Wall Carbon Nanotube Transistors

Jaan Männik, Iddo Heller, Anne M. Janssens, Serge G. Lemay, and Cees Dekker\*

*Kavli Institute of Nanoscience, Delft University of Technology, Lorentzweg 1, 2628 CJ Delft, The Netherlands*

Received December 14, 2007

## ABSTRACT

The noise properties of single-walled carbon nanotube transistors (SWNT-FETs) are essential for the performance of electronic circuits and sensors. Here, we investigate the mechanism responsible for the low-frequency noise in liquid-gated SWNT-FETs and its scaling with the length of the nanotube channel down to the nanometer scale. We show that the gate dependence of the noise amplitude provides strong evidence for a recently proposed charge-noise model. We find that the power of the charge noise scales as the inverse of the channel length of the SWNT-FET. Our measurements also show that surprisingly the ionic strength of the surrounding electrolyte has a minimal effect on the noise magnitude in SWNT-FETs.

Carbon nanotube-based transistors have attracted considerable interest as components of electronic circuits and sensors.<sup>1</sup> Inherent electrical noise determines the performance limits of these devices. The well-established high sensitivity of single-walled carbon nanotube transistors (SWNT-FETs) as biomolecular detectors<sup>2–4</sup> implicates that various fluctuating entities in the environment lead to a high level of noise in these devices. Understanding the origin and mechanism of this noise is essential to utilize SWNT-FET-based devices optimally and to improve them. For future applications in true nanoscale junctions, it is of interest to establish the scaling of the noise with the length of the SWNT down to the nanometer scale.

Extensive research on the noise properties of SWNT-FETs<sup>5–13</sup> has established that these transistors exhibit a  $1/f$ -type spectrum of noise in the low-frequency bandwidth where, for example, typical sensing measurements are performed. Typically, the noise spectra  $S_I(f)$  of the source-drain current  $I$  as a function of frequency  $f$  have been analyzed in the form

$$S_I(f) = A \frac{I^2}{f^\beta}$$

where  $\beta \approx 1$ , and  $A$  is the normalized noise amplitude. The dependence of the current spectral density  $S_I$  (or  $A$ ) on various parameters such as gate voltage<sup>7,12,14</sup>, nanotube length,<sup>7,8</sup> the substrate on which the SWNT rests,<sup>15</sup> and the

contact metal<sup>16</sup> has been discussed in the past. The majority of these studies compare experimentally measured noise magnitudes in SWNT-FETs<sup>5,7,12,14–16</sup> to the empirical Hooge model.<sup>17,18</sup> The latter states that  $A = \alpha/N_c$ , where  $N_c$  is the number of charge carriers in the nanotube, and  $\alpha$  is a constant. This model suggests that noise is caused by independent scattering events of charge carriers, which lead to a  $1/N_c$  dependence. Recently, Tersoff<sup>10</sup> has proposed an alternative model that assumes that the SWNT-FET is affected by random fluctuations of charge in its environment. In this so-called charge-noise model,  $S_I \propto (dI/dV_g)^2$  and  $A \propto (d(\ln(I))/dV_g)^2$ , as has been found also in other systems.<sup>19,20</sup> In this paper, we collect a reliable set of experimental data to compare to these two models and test their validity. We also discuss the effect that the electrolyte solution has on the noise properties of liquid-gated SWNT-FETs.

SWNTs were grown by chemical vapor deposition onto silicon wafers with a 500 nm thick SiO<sub>2</sub> layer. The typical diameters of these SWNTs as measured by atomic force microscopy (AFM) were 2.0 nm. The SWNTs were contacted with Au top electrodes with a thin 2.0 nm underlayer of Cr. SWNT transistors with a channel length below 100 nm were fabricated using an additional metal-evaporation step under a 45° angle.<sup>21</sup> For all measured SWNT-FETs (six devices in this study), it was verified by AFM that source and drain electrodes were connected by only a single nanotube. In typical measurements, the devices were immersed into 10 mM phosphate buffer (PB) solution at pH = 7.2. This solution was chosen because it corresponds to

\* Corresponding author. E-mail: c.dekker@tudelft.nl.

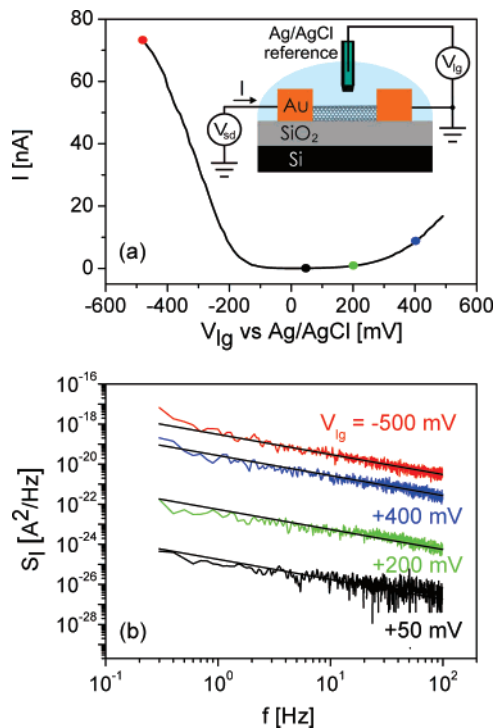


**Figure 1.** (a) SWNT-FET current versus liquid-gate potential referenced to Ag/AgCl electrode. Differently colored dots indicate the liquid-gate potentials at which noise measurements were recorded (see panel b). Inset: schematics of the measurements setup. (b) Current power spectral density as a function of frequency, measured at  $V_{lg} = -500, 50, 200,$  and  $400$  mV vs Ag/AgCl. The dashed lines represent fits to  $S_I(f) = S_I(1 \text{ Hz}) \cdot f_0/f$  where  $f_0 = 1 \text{ Hz}$ .

typical conditions of protein sensing measurements with SWNT-FETs. A liquid-gate potential was applied to an Ag/AgCl reference electrode in the flow cell (Figure 1a, inset).<sup>22</sup> A typical current versus liquid-gate voltage ( $V_{lg}$ ) curve is shown in Figure 1a. Both p-type conductance at negative voltages and n-type conductance at positive voltages can be seen in this measurement. Electrochemical currents due to the liquid gate, which were measured at source-drain potential  $V_{sd} = 0 \text{ V}$ , were subtracted from the source-drain currents, which were measured at  $V_{sd} = 10 \text{ mV}$ . These electrochemical currents remained small in the regions where the noise was measured (not exceeding 20% and typically much smaller), so that this procedure allowed us to extract the true source-drain current reliably (see Supporting Information). Similarly, the noise spectrum measured at  $V_{sd} = 0 \text{ V}$  was subtracted from the noise spectrum measured at  $V_{sd} = 10 \text{ mV}$ , to eliminate background amplifier noise and any possible noise related to the electrolytic currents (Figure 1b). The lowest measurable noise level in our setup was about  $10^{-27} \text{ A}^2/\text{Hz}$ .

Figure 2 shows measurements of the gate dependence of the source-drain current and the corresponding noise properties in 10 mM PB solution for three representative SWNT-FETs of different length. The shortest device of 60 nm length can be considered as a ballistic conductor, the 490 nm long device represents the quasi-ballistic regime, and the  $3.4 \mu\text{m}$  long device is in the diffusive regime of conductance, according to ref 23. The source-drain current as a function

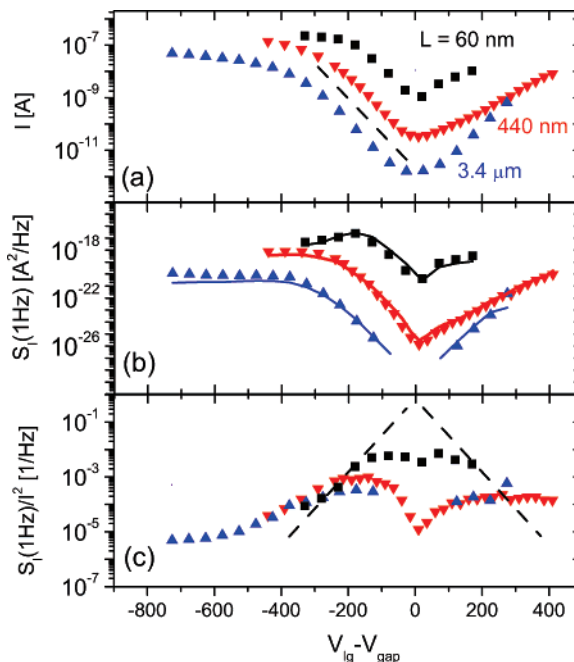


**Figure 2.** (a) Source-drain current vs liquid-gate potential for three SWNT-FETs. The channel lengths of these devices are 60 nm (■), 440 nm (▼), and  $3.4 \mu\text{m}$  (▲). The dashed line corresponds to a slope of 75 mV/decade. For better comparison, the curves of different devices have been horizontally shifted along the gate axes so that the zero volts corresponds to the minimum conductance of SWNT-FET. (b) Current noise power spectral density at 1 Hz frequency vs liquid-gate voltage for the same devices. Solid lines present a one-parameter fit to the charge-noise model. (c) Normalized noise amplitude  $A/f_0 = S_I/I^2$  at 1 Hz vs liquid-gate potential. The dashed lines correspond to a slope of  $+75$  and  $-75$  mV/decade, as expected for the Hooge model.

of liquid-gate potential shows an exponential dependence in the subthreshold regime with a 75 mV/decade slope in the p-type region (dashed line in Figure 2a). This type of behavior has been reported previously for similar devices.<sup>24</sup> Figure 2b shows measurements of the noise power spectral density at 1 Hz frequency,  $S_I(1 \text{ Hz})$ , for the same three devices. Earlier measurements of noise in SWNT-FETs have been performed in a limited range of gate voltages, either in the p-type or n-type conductance region. Here, we have been able to map out the noise in a much wider range of effective gate voltages, spanning from the p- to the n-type region in one measurement series. This has been possible due to the strong coupling of the gate field when we use the surrounding liquid as a gate electrode. As can be seen from Figure 2b,  $S_I$  varies significantly in the subthreshold regime for both the p- and n-type regions of conductance, whereas it is roughly constant in the ON-state of the device. Remarkably, the variation in  $S_I$  can be as large as 8 orders of magnitude.

We now compare the gate dependence of  $S_I$  to the Hooge and the charge noise models. To test the Hooge model for a wide range in  $V_{lg}$ , we plot  $A/f_0 = S_I(1 \text{ Hz})/I^2$  with  $f_0 = 1 \text{ Hz}$  in Figure 2c.<sup>25</sup> According to Hooge,  $A = \alpha/N_c$ , where  $N_c$  depends on the gate voltage.<sup>14</sup> We note two properties of  $N_c$  that hold irrespective of the ballistic or diffusive nature of electronic transport in SWNTs: (i)  $N_c$ , and thus  $S_I(1 \text{ Hz})/I^2$ , as a function of liquid-gate voltage follows an exponential

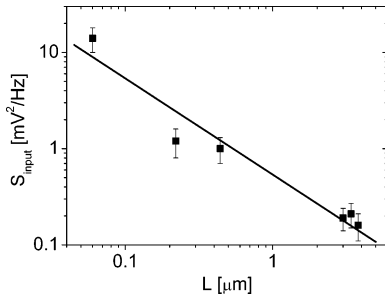


**Figure 3.** Input voltage noise,  $S_{\text{input}}$ , as a function of channel length of SWNT-FETs. The input noise is determined by fitting the noise power spectrum to  $S_{\text{input}}(dI/dV_{\text{lg}})^2$ , cf. Figure 2b. Solid line denotes  $S_{\text{input}} = 0.54[\text{mV}^2 \cdot \mu\text{m}/\text{Hz}]/L$ .

law in the subthreshold region with the same exponential slope as the source-drain current,<sup>10</sup> and (ii)  $N_c$  scales with the channel length as  $N_c \propto L$  at fixed gate voltage. Comparison to our noise measurements shows that the Hooge model fails to describe the data. The  $A$  versus  $V_{\text{lg}}$  dependence clearly does not reach the 75 mV/decade slope (dashed lines in Figure 2c) as observed in the  $I(V_{\text{lg}})$  curve. Moreover, the  $A$  versus  $V_{\text{lg}}$  curves of several devices show a well-defined local minimum at  $V_{\text{lg}} - V_{\text{gap}} = 0$ , where  $1/N_c$  should reach a maximum according to the Hooge model. It is also noticeable that all devices yield remarkably comparable  $A$  values that are quite independent of the length of the channel, except for the shortest device in the subthreshold region.

We now compare the data to the charge-noise model. The solid lines in Figure 2b are a fit of the charge-noise model that predicts  $S_I = S_{\text{input}}(dI/dV_{\text{lg}})^2$  where the fitting parameter,  $S_{\text{input}}$ , refers to the noise-power spectral density at the liquid-gate capacitor, that is, at the input terminal of the device. For the fits,  $dI/dV_{\text{lg}}$  is obtained from the experimentally measured  $I(V_{\text{lg}})$  curve (Figure 2a) using numerical differentiation. The only parameter left,  $S_{\text{input}}$ , is found by fitting the data in the subthreshold region of  $V_{\text{lg}}$  values. The parameter  $S_{\text{input}}$  shifts the experimentally determined fitting function  $(dI/dV_{\text{lg}})^2$  up or down in the logarithmic plot without changing the shape of the curve. Although the fit deviates somewhat from the data in the p-type region for the largest ON-state currents, it closely follows the data for almost 6 orders of magnitude variation in  $S_I$  for lower currents. From this, we conclude that the charge-noise model presents an accurate description of our data in the subthreshold regime of SWNT-FETs.

Having shown that the charge-noise model captures the gate dependence of the noise power well, we now further investigate the underlying mechanism. Figure 3 displays the fitting parameter  $S_{\text{input}}$  as a function of nanotube length. As one can see, the level of charge noise is higher for SWNT-FETs with short nanotube lengths. Indeed, it appears that  $S_{\text{input}} \propto 1/L$ . How can this length dependence be explained? In the charge-noise model, the voltage fluctuations of the gate, described by  $S_{\text{input}}$ , are the result of charge fluctuations. These fluctuations couple to the SWNT-FET through some effective gate capacitance,  $C_{\text{gate}}$ , so that

$$S_{\text{input}} = (dV_{\text{lg}}/dq)^2 S_q = (1/C_{\text{gate}})^2 S_q$$

The effective gate capacitance scales as  $C_{\text{gate}} \propto L$  and is presumably dominated by the quantum capacitance.<sup>24</sup> On the other hand, a homogeneous distribution of independent charge fluctuators along the length of the SWNT leads to  $S_q \propto L$ . Combining these dependencies for  $C_{\text{gate}}$  and  $S_q$  gives  $S_{\text{input}} \propto 1/L$ , as indeed observed in Figure 3.

To further investigate the generality of the conclusions we have drawn, we studied the salt dependence of the noise magnitude. Figure 4 shows  $S_I(V_{\text{lg}})$  in three very different salt concentrations as well as in air for a single SWNT-FET device. The straightforward conclusion from the data is that the ionic strength of the solution does not affect the noise magnitude (for a more extensive set of electrolytes, see Supporting Information). This result agrees with measurements of nanotube mats in electrolytes.<sup>12</sup> Figure 4 shows that the noise levels do not change significantly even when the environment is air instead of electrolyte, as the levels of  $S_I$  in the ON- and OFF-states in air and in electrolyte are almost the same. Unfortunately, it is difficult to carefully verify  $S_I \propto (dI/dV_{\text{lg}})^2$  in air because of hysteresis and drift commonly observed in the gate curves of these devices in ambient air.

It is often thought that charge noise originates from the  $\text{SiO}_2$  substrate underneath the devices. Because a higher ionic strength corresponds to more screening of the surface charges, variation of the ionic strength should yield information on the length scale over which fluctuators induce noise in the conductance of SWNT-FETs. We observe shifts in the  $I(V_{\text{lg}})$  curves (inset of Figure 4) that are consistent with the idea of gating of SWNT-FETs by the negative surface charge of  $\text{SiO}_2$  and more efficient screening of this surface charge at higher ionic strengths. For the three electrolytes presented in Figure 4, the Debye screening length can be estimated to be 0.7 nm (100 mM KCl plus 10 mM PB), 1.1 nm (10 mM PB) and  $>30$  nm (deionized water, DI). Interestingly, however, despite large variation in the screening lengths, we observe no change in the noise properties.

The data of Figure 4 lead us to conclude that the bulk of the substrate that is more than  $\sim 1$  nm away from the SWNT in the lateral direction contributes little to the noise of SWNT-FETs. The  $S_{\text{input}} \propto 1/L$  dependence as discussed before, also excludes that charge fluctuations in the SWNT-metal contacts are the dominating source of noise. Together these statements imply that the charge fluctuators reside in the immediate vicinity of the SWNT either in the silicon oxide layer directly underneath SWNT or as adsorbates on the nanotube surface. The latter has been suggested before.<sup>5,7,12</sup>

As can be seen from Figure 2b, the charge noise model does not give a perfect fit to the data in the ON-state far away from the subthreshold region and in particular for longer SWNTs where transport of charge carriers is diffusive.<sup>7</sup> In this region of gate voltages, it is likely that a different noise mechanism takes over. Tersoff<sup>10</sup> has proposed to include an extra term in the noise expression similar to the Hooge model, viz.,  $S_I = S_{\text{input}}(dI/dV_{\text{lg}})^2 + A I^2$ . This indeed

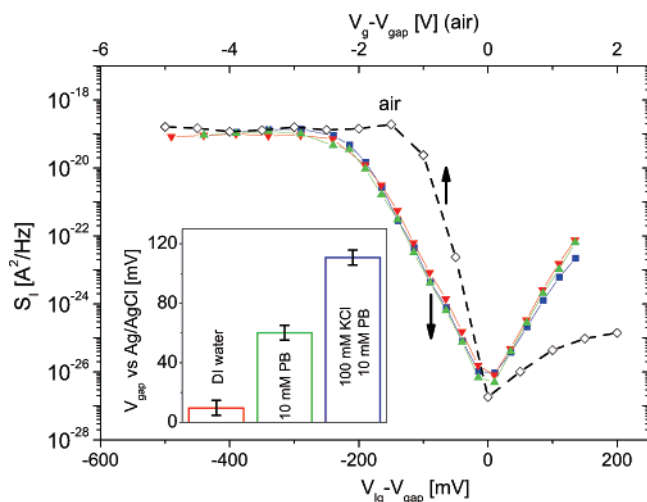


**Figure 4.** Noise spectral density  $S_1$  (1 Hz) vs  $V_{lg}$  in different electrolytic solutions (bottom horizontal axis) and in air (top horizontal axis). The electrolytic solutions used are DI water ( $\blacktriangledown$ ), 10 mM PB solution ( $\blacktriangle$ ), and 100 mM KCl solution in 10 mM PB ( $\blacksquare$ ). Lines connecting the points are guides to the eye. Curves measured in electrolyte solutions are shifted relative to Ag/AgCl reference electrode by the amount shown in the inset.

provides a better fit to our data in the ON-state (see Supporting Information Figure S3).

Our measurements have clear implications for the design of SWNT-FET biosensors. Here, we will discuss the sensitivity of detecting (i) a single protein-adsorption event and (ii) the lowest analyte concentrations by using SWNT-FETs. In both cases, we assume that the sensing mechanism for biomolecule detection is electrostatic gating by the charges of biomolecules,<sup>26</sup> which leads to a response curve proportional to  $dI/dq = (1/C_{gate})dI/dV_{lg}$ . For case (i), the signal-to-noise ratio for single-molecule detection is proportional to  $[(1/C_{gate})dI/dV_{lg}]/S_1^{1/2}$ , which according to our earlier arguments scales as  $L^{-1/2}$ . Thus, to detect a single molecule adsorption event, a SWNT-FET with the shortest channel length should be used. For case (ii) however, we estimate the signal-to-noise ratio by assuming that the analyte is deposited uniformly along the length to SWNT and that the total number of analyte molecules on the nanotube is thus proportional to the length of SWNT. This leads to scaling of signal-to-noise ratio as  $L^{1/2}$ , that is, a SWNT-FET with a longer channel length should be used.

In conclusion, we have shown that charge noise  $S_1 \propto (dI/dV_{lg})^2$  dominates the noise of SWNT-FETs in the subthreshold region where these devices are commonly used as electronic components and sensors. The level of this noise scales as the inverse of SWNT length. The microscopic origin of this noise requires further investigation, but the bulk of surface oxide, which is in the lateral direction more than  $\sim 1$  nm away from the SWNT, does not significantly contribute to the noise.

**Acknowledgment.** The authors thank E. D. Minot and H. A. Heering for useful discussions. This work was supported in part by FOM, NanoNed, NWO.

**Supporting Information Available:** Current measurements in electrolytic environment, noise measurements in extended set of electrolytes, and fitting of noise data with the combined charge noise and Hooge's model. This material is available free of charge via the Internet at <http://pubs.acs.org>.

## References

- (1) *Applied Physics of Carbon Nanotubes*; Rotkin, S.V., Subramoney, S., Eds.; Springer-Verlag: Berlin, 2005.
- (2) Chen, R. J.; Bangsaruntip, S.; Drouvalakis, K. A.; Kam, N. W. S.; Shim, M.; Li, Y. M.; Kim, W.; Utz, P. J.; Dai, H. J. *Proc. Nat. Acad. Sci. U.S.A.* **2003**, *100*, 4984.
- (3) Besteman, K.; Lee, J. O.; Wiertz, F. G. M.; Heering, H. A.; Dekker, C. *Nano Lett.* **2003**, *3*, 727.
- (4) Allen, B. L.; Kichambare, P. D.; Star, A. *Adv. Mat.* **2007**, *19*, 1439.
- (5) Collins, P. G.; Fuhrer, M. S.; Zettl, A. *Appl. Phys. Lett.* **2000**, *76*, 894.
- (6) Postma, H.W.C.; Teepen, T.F.; Yao, Z.; Dekker, C. *1/f Noise in Carbon Nanotubes*. In *Proceedings of XXXVIIth Recontre De Moriond*; EDP Sciences: Les Ulis, France, 2001.
- (7) Ishigami, M.; Chen, J. H.; Williams, E. D.; Tobias, D.; Chen, Y. F.; Fuhrer, M. S. *Appl. Phys. Lett.* **2006**, *88*, 203116.
- (8) Lin, Y. M.; Appenzeller, J.; Chen, Z. H.; Avouris, P. *Phys. E* **2007**, *37*, 72.
- (9) Snow, E. S.; Novak, J. P.; Lay, M. D.; Perkins, F. K. *Appl. Phys. Lett.* **2004**, *85*, 4172.
- (10) Tersoff, J. *Nano Lett.* **2007**, *7*, 194.
- (11) Reza, S.; Huynh, Q. T.; Bosman, G.; Sippel-Oakley, J.; Rinzler, A. G. *J. Appl. Phys.* **2006**, *100*, 094318.
- (12) Briman, M.; Bradley, K.; Gruner, G. *J. Appl. Phys.* **2006**, *100*, 013505.
- (13) Peng, H. B.; Hughes, M. E.; Golovchenko, J. A. *Appl. Phys. Lett.* **2006**, *89*, 243502.
- (14) Lin, Y. M.; Appenzeller, J.; Knoch, J.; Chen, Z. H.; Avouris, P. *Nano Lett.* **2006**, *6*, 930.
- (15) Lin, Y. M.; Tsang, J. C.; Freitag, M.; Avouris, P. *Nanotechnology* **2007**, *18*, 295202.
- (16) Appenzeller, J.; Lin, Y. M.; Knoch, J.; Chen, Z. H.; Avouris, P. *IEEE Trans. Nanotechnol.* **2007**, *6*, 368.
- (17) Hooge, F. N. *Phys. Lett. A* **1969**, *A 29*, 139.
- (18) Hooge, F. N. *IEEE Trans. Electron Devices* **1994**, *41*, 1926.
- (19) Dekker, C.; Scholten, A. J.; Liefvink, F.; Eppenga, R.; Vanhouten, H.; Foxon, C. T. *Phys. Rev. Lett.* **1991**, *66*, 2148.
- (20) Zimmerli, G.; Eiles, T. M.; Kautz, R. L.; Martinis, J. M. *Appl. Phys. Lett.* **1992**, *61*, 237.
- (21) Javey, A.; Qi, P. F.; Wang, Q.; Dai, H. J. *Proc. Nat. Acad. Sci. U.S.A.* **2004**, *101*, 13408.
- (22) Minot, E. D.; Janssens, A. M.; Heller, I.; Heering, H. A.; Dekker, C.; Lemay, S. G. *Appl. Phys. Lett.* **2007**, *91*, 093507.
- (23) Javey, A.; Guo, J.; Wang, Q.; Lundstrom, M.; Dai, H. J. *Nature* **2003**, *424*, 654.
- (24) Rosenblatt, S.; Yaish, Y.; Park, J.; Gore, J.; Sazonova, V.; McEuen, P. L. *Nano Lett.* **2002**, *2*, 869.
- (25) In several earlier publications,  $A$  has dimensions  $1/\text{Hz}^{1-\beta}$ . We, however, use  $A = S(1 \text{ Hz}) * f_0 / I^2$  where  $A$  is dimensionless.
- (26) Heller, I.; Janssens, A. M.; Männik, J.; Minot, E. D.; Lemay, S. G.; Dekker, C. *Nano Lett.*, in press.

NL073271H